Studies of the radon progeny particle size distributions in the domestic environment. Epidemiological and dosimetric dose estimates

Kalina Mamont-Cieśla,
Olga Stawarz

Abstract. Measurements of the short-lived radon progeny particle size distributions were performed under realistic natural conditions in 54 dwellings in 6 regions of Poland by means of the Radon Progeny Particle Size Spectrometer (RPPSS). The RPPSS comprises a one open face stage, a 4-stage diffusion battery and a 3-stage multi-hole inertial impactor. It was manufactured at the ARPaNSA (Melbourne, Australia), under supervision of Dr S. B. Solomon and supplied with his software. While using the continuous mode, the programme provides analysis of the potential alpha energy concentration on each stage, particle size distributions and weighted dose conversion factors based on the ICRP human respiratory tract model (HRTM) as implemented in the computer code RADEP (radon dose evaluation program). The unattached fraction indoors ranges from ca. 0 to 53% with an arithmetic mean and median of 17%. The equilibrium factor F was observed in the range from 7 to 64% with an arithmetic mean of 32% and median of 29%. The annual effective doses from radon progeny for the general population were estimated according to two models: epidemiological and dosimetric. The mean values of the ratios of the dosimetric to epidemiological dose estimates for the general population (breathing rate 0.78 m^3/h) and workers (breathing rate 1.2 m^3/h) are 1.0 and 1.4, respectively. The epidemiological dose estimates for the general population are smaller in comparison with the dosimetric estimates for the unattached fraction f_p greater than 17%. It was shown that the dependence of the ratio of the doses estimated on the basis of two models on the unattached fraction f_p is well described by a linear equation.

Key words: radon progeny particle size distribution (RPPSD) • weighted dose conversion factors • dosimetric/epidemiological effective dose estimate • conversion convention • unattached fraction (f_p) • radon dose evaluation program (RADEP)

K. Mamont-Cieśla✉, O. Stawarz
Central Laboratory for Radiological Protection,
7 Konwaliowa Str., 03-194 Warsaw, Poland,
Tel.: +48 22 814 0159, Fax: +48 22 811 1616,
E-mail: kalinam@clor.waw.pl

Introduction

Atoms of the radon daughters immediately after the radioactive decay of radon atoms have tendency to attach to condensation nuclei producing radioactive aerosols. Aerosols of size below 10 nm, composed of unattached ions or neutral atoms and molecular clusters associated with radon progeny atoms, are traditionally called unattached fraction. Aerosols above 10 nm up to greater than 1000 nm, with a predominant size between 50 and 500 nm, are called attached fraction. It is estimated that equivalent dose to the lung from radon gas is only about one hundredth of that from its short-lived daughters which constitute the main health hazard to the human respiratory tract in the radon environment. The effective dose, a measure of this hazard, is calculated as a product of the potential alpha energy concentration (PAEC) in the air and a dose conversion factor (DCF) or dose per unit intake.

There are two approaches to the estimation of DCF. One of them, recommended by the International Radiation Protection Committee Publication 65 [5] introduces

two single conversion factors, called radon progeny conversion convention, 1425 mSv/(J·h/m³) for the occupational hazard and 1100 mSv/(J·h/m³) for the general population. The conversion factors are determined from the epidemiological studies of uranium miners.

A second, biokinetic and dosimetric approach is based on the ICRP Publication 66 [6] which strongly recommends the usage of the human respiratory tract model (HRTM) for inhalation of airborne radionuclides. The dosimetric models reveal that the dose per the unit of intake of radon progeny depends on the radon progeny aerosol characteristics, in particular, on the size and fraction of the ultrafine atoms and clusters (unattached fraction) and the physiological parameters such as the breathing rate. The site of the aerosol deposition in the respiratory tract strongly depends on the particle size distribution. Because diffusion is the dominating mechanism of the aerosol deposition in the lung, the most diffusive fraction, mostly the first radon progeny ^{218}Po, constitutes the biggest cancer risk. Therefore, it is particularly important for the estimation of the radon effective dose to measure the particle size distribution. The dosimetric approach uses the weighted dose conversion factor which combines the radon progeny size distribution in a particular exposure location with the particle-size dependent dose conversion factors derived from ICRP Publication 66. The dosimetric models adopt the assigned fraction of the tissue weighting factor w_T for the lung and the radiation weighting factor w_R for alpha radiation.

Some authors [13, 18] indicate that particularly in the domestic environment in well ventilated homes where the unattached fraction of potential alpha energy can be relatively high, on the contrary to mines, the radon dose estimations using two models may significantly differ.

The main objective of this paper was to measure the radon progeny particle size distributions and potential alpha energy concentrations in the realistic domestic environment in various natural radon and aerosol conditions and to estimate the annual effective doses to inhabitants of the investigated houses by means of two approaches: epidemiological and dosimetric. In the studied houses the radon concentrations were simultaneously measured to calculate the equilibrium factor F.

Methods and materials

Measurements indoors and outdoors

The measurements were performed in the buildings selected accidentally in six regions of Poland: in the mountains in the vicinity of Jelenia Góra and Szczawno Zdrój, in the rural areas near Białystok, in the flat areas near Leżajsk and Leszno Wielkopolskie and in towns: Warszawa and Wałbrzych. The measurements were made in various seasons of the year, during daytime and in night, in houses of smokers, in well ventilated houses, in the conditions of the high (from frying and boiling of meals) and low levels of aerosols. Selection of houses was casual and depended on getting permission of the inhabitants for installing a big and

annoying laboratory in their houses. The measurements were lasting at least 5 h. In some cases it was possible to make longer measurements. The same measurements were planned to be performed outdoors nearby the house. In each case, simultaneously with the measurements of the PAEC and the radon daughter size distributions, the radon concentration was measured by an AlphaGUARD monitor, manufactured by Genitron (Germany) to estimate the equilibrium factor F. The PAEC and size distribution of the radioactive aerosols were measured by means of a unique instrument – a radon progeny particle size spectrometer, manufactured in the ARPaNSA (Melbourne, Australia) [14] supplied with software developed by Dr S. B. Solomon and distributed by ACJ&Associates, Inc. USA.

Description of the Radon Progeny Particle Size Spectrometer [14]

The Radon Progeny Particle Size Spectrometer Mk2 (RPPSS) in the configuration for the field measurements in the continuous mode comprises the following main components: the 8-stage sampling head (one open face stage, 4-stage wire screen diffusion battery and 3-single stage multi-hole inertial impactor system), the power supply/12-channel counter unit, the oil-free vacuum pump, the notebook.

The schematic modular diagram and sampling configuration of the RPPSS are drawn in Fig. 1. The sampling head consists of a one open face stage, four stage wire screen diffusion battery system, three single stage multi-hole inertial impactor system and a sampling manifold comprising eight inlets and one outlet. All eight stages operate in parallel and simultaneously. Each stage uses a detector housing with a PIP CAM 400 detector of the surface of 450 mm² (24 mm dia.) and an aluminum holder to suit 47 mm dia. membrane filter or impaction plate. In the first stage, with an open filter, the total activity collected from the air flown through is measured. In the four consecutive stages the filters collect only these particles which were not stopped by sets of wire screens preceding them in the stream of the measured air. In the last three stages thin aluminized mylar foils are positioned in place of the filters which play a role of the impaction surfaces of the multi-hole inertial impactor. The alpha particles emitted by aerosols impacted onto the impactor surfaces pass through the mylar to the detector. The characteristics of the
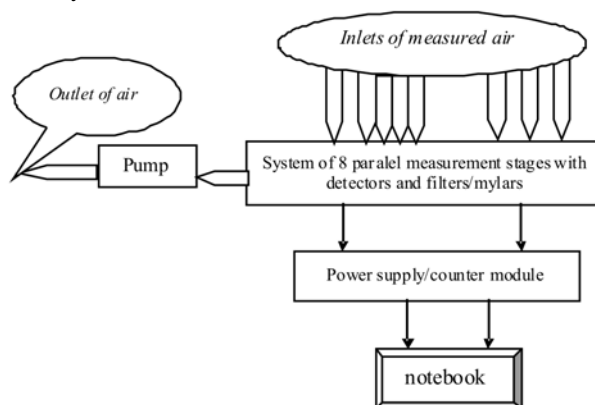
Fig. 1. Diagram of the RPPSS – configuration for field measurements.

Table 1. Characteristics of the diffusion battery stages in the RPPSS[a]

No. of stage	#1	#2	#3	#4	#5
Type of screen	–	A	A	A	B
Number of screens	–	1	2	13	32
Mesh numbers	–	100	100	100	200
Screen diameter (cm)	–	1.7	3.8	3.8	3.8
Wire diameter (μm)	–	112	112	112	35
Wire thickness (μm)	–	215	215	215	80
Solid fraction of screen (%)	–	31.3	31.3	31.3	29.1
Dp50 (nm)	–	1.2	4.3	17.3	72.3
Counting efficiency (%)	12.80	13.0	13.0	13.0	13.0
Flow rate (lpm)	4.15	4.45	4.25	4.20	4.25

[a] RPPSS – Radon Progeny Particie Size Spectrometer.

Table 2. Characteristics of the impactor stages in the RPPSS[a]

No. of stage	#6	#7	#8
Number of holes	3	7	1
Dp50 (nm)	316	522	1096
Dp50 lower bound (nm)	250	500	1000
Dp50 upper bound (nm)	350	700	1400
Function slope	1.23	3.30	6.00
Function intercept	2.02	2.25	2.20
Counting efficiency (%)	21.4	21.8	21.8
Flow rate (lpm)	3.45	2.90	3.30

[a] RPPSS – Radon Progeny Particie Size Spectrometer.

diffusion battery and impactor are given in Tables 1 and 2, respectively. The sampling head also comprises a sampling manifold with five inlets containing critical orifices to set the flow at ca. 4 lpm (in the first five stages) and three inlets containing critical orifices to set the flow at ca. 3 lpm. Every time before a series of the field measurements the flow rate at each stage is checked and may be corrected in the program, if needed. The field measurements are performed in the continuous mode of work which is controlled by a PC-based program. It is designed to collect data from all eight stages simultaneously. It integrates the full α particle energy spectrum for each stage to provide gross-alpha counts over a set time interval. The integrated counts are converted to the radon progeny potential α energy concentration using the effective energy radon progeny of 7.2 MeV (1.152×10^{-3} nJ) and taking into account the flow rate, detector efficiency, background and time of counting. Thus, the concentration of the radon progeny is calculated by the following formula: PAEC = $k \cdot N$, where PAEC is the potential α energy concentration in nJ/m³, N are the counts per unit of time in cpm, k is the conversion factor in nJ·min/m³ calculated as: $k = 1.152/(v \cdot eff)$ where v is the flow rate in l/min, eff is the α counting efficiency of the detector. The systematic uncertainties associated with the conversion of gross-alpha counts to PAEC are usually less than 5% if the PAEC levels are about stable, but the conversion is less accurate when the PAEC is varying rapidly [14].

Uncertainty of the conversion factor k is usually less than 5%. The low level of detection (LLD) for PAEC is ca. 25 nJ/m³ with uncertainty of 30% at ca. 95% confidence level.

As it was said above, the first stage with a bare filter delivers data on the total PAEC, carried out by both attached and unattached radon daughters. The program corrects for plateout of ultrafine radon daughters in the inlet tube to the first stage. There is no correction for a possible thoron daughter contribution. The program calculates the dependence of the particle penetration efficiency on the size of particles according to the fan-filtration theory of Y. S. Cheng and H. C. Yeh [4] and Y. S. Cheng et al. [3] for the screen type diffussion battery. For the impactor stages, the theory developed for cascade impactors by V. A. Marple and K. L. Rubow [10] was modified and applied. The program calculates the penetration matrix for 43 equi-logspaced size intervals between 0.6 nm and 2494 nm. Equivalent diffusion (thermodynamic) diameters are used for the wire screen stages and equivalent impaction (aerodynamic) diameters are used for the impactor stages. The latter are matched to the thermodynamic diameters using a particle density dependent function. For the value of the unit density, the diameters are the same. The derived PAEC values for each stage are used as input values to two independent deconvolution algorithms, one developed by S. Twomey [17] (TWOMEY) and another one called "Expectation Maximization" (EMAX) by E. F. Maher and N. M. Laird [9]. The deconvolution analysis results in the radon progeny particle size distribution. It derives for each mode: the geometric mean diameter (activity median aerodynamic diameter-AMAD in nm), geometric standard deviation and the percentage contribution to the potential alpha energy concentration.

In order to calculate the size-weighted DCF for the obtained particle size distribution in the sampled air the program applies the ICRP 66 Respiratory Tract Model implemented in the computer program RADEP (radon dose evaluation program) by A. Birchall and A. C. James [1]. The dependence of the DCF for an adult male with breathing rates of 1.2 m³/h (hard working) and 0.78 m³/h (general population) on the particle diameter applied in this program is shown in Fig. 2. It was assumed that the representative activity concentration ratios for ^{218}Po:^{214}Pb:^{214}Bi is 0.8:0.02:0.0 and 0.8:0.4:0.2, for particle sizes < 20 nm and $\geq$ 20 nm, respectively. Figure 2 shows that the dose per unit exposure (DCF) is about a factor of 25 times higher for the particle size of ca. 1 nm (the unattached fraction) than for the particle size in the range 100–300 nm (the attached fraction).

The RADEP-derived DCF values are normalized by a factor of 0.3 [8] to provide consistency with the results
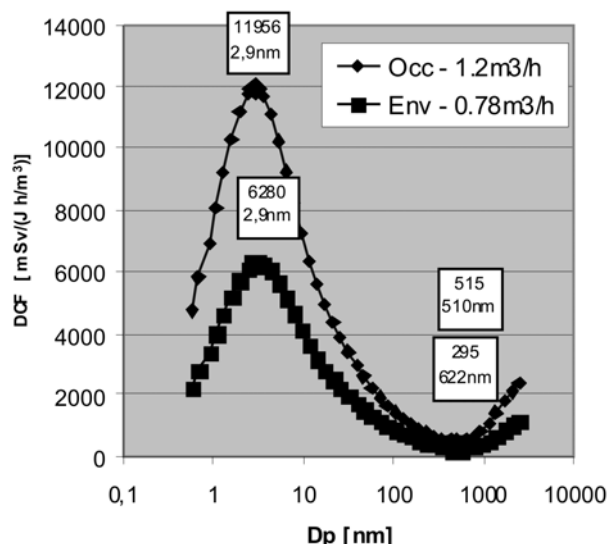
Fig. 2. The dependence of the DCF on the particle diameter dp for monodispersed particles. Assumptions: ratio of activity concentration: ^{218}Po:^{214}Pb:^{214}Bi of 0.8:0.02:0.0 for dp < 20 nm and of 0.8:0.4:0.2 for dp ≥ 20 nm.

Fig. 3. The collection efficiency curves for all 8 stages in the RPPSS.

derived from the epidemiological risk estimate with the use of the ICRP 65 conversion convention. This factor was chosen to match the RADEP-derived DCF values to the ICRP 65 conversion convention for the uranium mine aerosol conditions. It will be discussed in section 'Summary' of this paper.

The program applies the collection efficiency curves for the eight stages, in the diameter range from 0.6 to 2496 nm which are shown in Fig. 3.

Before and after each series of measurements the flow rate and counting efficiency at each of eight stages were checked. The counting efficiency stability was verified by means of a control Pu-239 source placed instead of the filter in the diffusion battery (DB) stages and the mylar foil in the impactors. In Tables 1 and 2 characteristics of all stages and typical values of the flow rate are presented.

The measurements performed in a Central Laboratory for Radiological Protection (CLOR, Warsaw, Poland) radon chamber in two kinds of aerosol conditions: low aerosols (< 200 CN/cm³) and high aerosols (ca. 20 000 CN/cm³), (CN – condensation nuclei), revealed good consistency between results obtained by means of two algorithms: TWOMEY and EMAX. Comparison of the DCF and the particle size distributions calculated by two algorithms for the low and high aerosol conditions in the CLOR radon chamber are given in Table 3.

According to the estimation made by S. B. Solomon [13, 14] the uncertainty of the DCFs for the polidispersion size distribution reaches ± 10% for workers and ± 20% for the general population.

The annual effective doses from radon progeny

During the measurements, the program every hour delivers PAEC values and two values of the DCF for each of two algorithms: DCF Env for the general population and DCF Occ for hard working men. To assess the an-

Table 3. Comparison of the DCFs and the particle size distributions delivered by two algorithms EMAX and TWOMEY for low (< 200 CN/cm³) and high (ca. 20 000 CN/cm³) aerosol conditions in the CLOR radon chamber

< 200 CN/cm³		General population	Workers	
EMAX	DCF	2086	4364	
TWOMEY	DCF	2294	4781	
		Mode #1	Mode #2	Mode #3
EMAX	GMD[b] (nm)	0.7	418	1378
Contribution	(%)	87	3	10
TWOMEY	GMD (nm)	0.6	343	1375
Contribution	(%)	84	5	11
20 000 CN/cm³		General population	Workers	
EMAX	DCF	579	983	
TWOMEY	DCF	629	1069	
		Mode #1	Mode #2	Mode #3
EMAX	GMD[b] (nm)	1.1	157	730
Contribution	(%)	0.07	91	9
TWOMEY	GMD (nm)	1.3	169	761
Contribution	(%)	0.04	92	8

[a] CN – condensation nuclei.
[b] GMD – geometric median diameter.

Table 4. The particle size distributions indoors

Name of place	Mode #1			Mode #2			Mode #3		
	GMD[a] (nm)	GSD[b]	U[c] (%)	GMD (nm)	GSD	U (%)	GMD (nm)	GSD	U (%)
BukGaj4K a	0.7; 8	1.4	46	166	1.9	48	1345	1.4	6.3
BukGaj4K b	0.8; 6	1.6	16	139	1.9	77	878	1.5	7.0
BukGaj4P a	0.8	1.7	12	158	1.9	85	1236	1.4	2.8
BukGaj4P b	0.8	1.6	22	208	2.0	78	–	–	–
BukGaj3K a	0.7	1.4	18	154	1.7	73	685	1.4	9.6
BukGaj3K b	0.8	1.7	29	199	2.1	71	–	–	–
BukGaj3 S	0.7	1.4	22	207	1.9	78	–	–	–
Kurosiówka a	0.8	1.6	14	149	1.6	81	813	1.5	5.2
Kurosiówka b	0.7	1.4	20	154	1.7	73	743	1.5	7.4
SzlarskaP	0.8	1.5	27	156	1.7	68	884	1.5	5.0
Borowice	0.7	1.4	17	128	2.0	77	685	1.5	6.5
Grodzisko	0.8	1.3	48	187	1.3	56	1592	1.3	2.5
Leszno Gierym.	0.9	1.4	21	167	1.4	75	835	1.4	5.0
Leszno Olsz.	1.0	1.4	32	165	1.4	62	–	–	–
Lipno	0.8	1.6	27	150	1.5	70	1086	1.4	2.7
Osieczna	0.8	1.3	30	169	1.4	70	939	1.5	6.6
Poniec Dom	–	–	–	179	1.4	92	631	1.3	8.0
Poniec war.	0.9	1.4	16	172	1.3	78	660	1.4	6.0
Rokosowo	0.8	1.3	27	173	1.4	69	851	1.4	3.8
Michałów 1	1.0	1.7	5	130	1.6	92	724	1.1	3.0
Michałów 2	0.7	1.3	11	144	1.4	78	774	1.2	11.0
Studzianki 1	0.8	1.3	24	170	1.3	70	847	1.3	6.0
Studzianki 2a	1.0	1.6	15	145	1.5	81	752	1.2	5.0
Studzianki 2b	1.1	1.8	1	121	1.7	97	747	1.2	2.1
Studzianki 3a	0.8	1.4	10	139	1.4	82	773	1.1	8.1
Studzianki 3b	0.8	1.4	0.2	136	1.4	91	780	1.1	9.0
Giedlarowa	0.8	1.4	17	124	1.9	81	778	1.5	2.0
Grodzisko a	0.7	1.4	17	129	1.8	80	817	1.6	3.5
Grodzisko b	0.8	1.4	9	130	1.7	89	700	1.4	3.0
Gielershof	0.8	1.3	16	184	1.8	84	–	–	–
Leżajsk Rynek	0.8	1.5	20	133	2.3	81	–	–	–
Wałbrzych 1	5.9	1.8	2	135	1.6	94	888	1.3	4.8
Wałbrzych 2a	0.8	1.5	6	147	1.5	89	789	1.3	5.3
Wałbrzych 2b	0.7	1.6	13	142	1.5	83	849	1.4	5.0
Wałbrzych 3	0.7	1.4	11	147	1.4	86	923	1.4	3.0
Szczawno	0.7	1.3	12	152	1.5	85	1007	1.4	3.1
Janowice 1a	0.7	1.2	7	140	1.4	90	1009	1.2	3.2
Janowice 1b	0.6	1.2	17	151	1.4	79	909	1.2	4.3
Janowice 2a	0.7	1.2	13	143	1.4	82	1042	1.3	6.0
Janowice 2b	0.6	1.2	19	130	1.3	75	1030	1.3	5.6
Syta2	0.2	1.7	19	134	1.5	78	1011	1.3	2.9
Wilanów a	2.0	2.1	25	155	1.7	68	789	1.5	7.2
Wilanów b	1.1	1.7	4	172	1.4	85	753	1.3	11.0
Służew a	1.1	1.8	25	157	1.6	68	789	1.4	7.2
Służew b	1.9	2.5	17	145	1.8	72	660	1.3	3.0
Wesoła a	0.1	2.0	20	134	1.7	74	794	1.3	6.0
Wesoła b	1.0	1.7	12	145	1.5	82	1110	1.4	6.4
Bemowo a	0.7	1.4	53	123	2.8	40	919	1.7	7.0
Bemowo b	1.2	1.6	16	138	1.6	79	895	1.2	5.6
Ochota a	0.6	1.2	30	153	2.1	70	1361	1.4	1.6
Ochota b	0.6	1.2	19	141	1.8	80	655	1.3	2.5
Śródmieście a	1.0	1.7	10	151	1.5	80	721	1.2	9.7
Śródmieście b	1.4	1.8	1	152	1.5	88	713	1.2	11.0
Żerań a	1.0	1.6	1	156	1.5	91	709	1.4	7.8
Żerań b	0.9	1.7	6	160	1.4	80	755	1.2	14.0
Arithmetic mean	**0.9**	**1.5**	**18**	**152**	**1.6**	**78**	**874**	**1.4**	**6.0**

[a] GMD – geometric mean diameter.
[b] GSD – geometric standard deviation.
[c] U – percentage contribution.
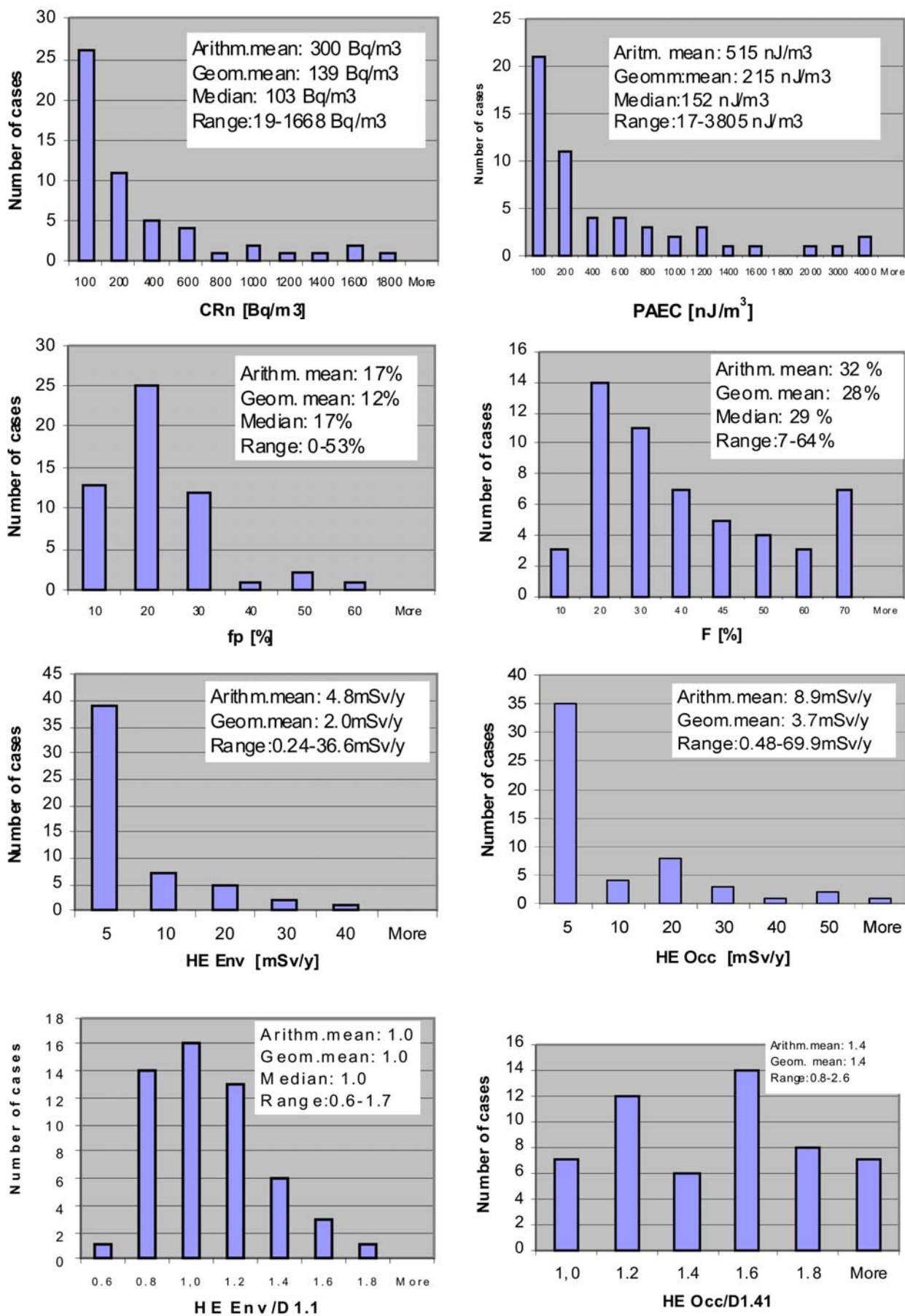
Fig. 4. Histograms of the radon concentrations C_{Rn}, PAEC, unattached fractions f_p, equilibrium factors F, dosimetric doses: HE Env and HE Occ and ratios of the dosimetric to epidemiological dose for the general public and hard working men, indoors.

nual effective doses in the tested rooms the EMAX DCF values were used. Although the main objective of this paper is indoor doses to the general population, there are also calculated doses to the hard working adult men in the same radon and aerosol conditions to compare the differences between dosimetric and epidemiological dose estimates in the two cohorts.

The doses estimated for two models were calculated according to the following formulae:
– for the dosimetric model: HE Occ = PAEC·DCF Occ·t and HE Env = PAEC·DCF Env·t
– for the epidemiological model: D Occ = PAEC·1425·t and D Env = PAEC·1100·t

where: HE Occ, HE Env, D Occ and D Env are in mSv/y, PAEC in nJ/m^3, DCF Occ and DCF Env in mSv/(J·h/m^3) and t = 8760 h/y.

Results and discussion

Altogether in six regions of Poland there were gathered results in 54 houses and only four results in the outdoor atmosphere because in the most of the outdoor measurements the statistics was too low to deliver reliable results.

In Table 4 there are given the following characteristics of the particle size distributions indoors: the geometric mean diameter (GMD), the geometric standard deviation (GSD) and the percentage contribution (U) of each mode to the distribution for each measurement site. In the majority of cases three modes appear: mode #1, corresponding to the unattached fraction f_p, of GMD in the range: 0.2–8 nm, mode #2, corresponding to the dominating ambient fraction in the distribution, of GMD in the range from 98 to 208 nm and mode #3, corresponding to the biggest particles, of GMD in the range from 631 to 1532 nm. The mode #2 with arithmetic means of the GMD, GSD and U equal to 152 nm, 1.6 and 78% and mode #3 with arithmetic means of the GMD, GSD and U equal to 874 nm, 1.4 and 6% make the attached fraction. Only in three sites appeared two modes #1 and #2 and in one site mode #2 and mode #3.

Values of the GSD of the diameters for all three modes range from 1 to 2 in the majority of cases. In only 5 cases they slightly exceed 2.

In Fig. 4 there are frequency distributions of the obtained results of the radon concentration C_{Rn}, potential alpha energy concentration PAEC, equilibrium coefficient F, unattached fraction f_p, dosimetric doses: HE Env and HE Occ and ratios of the effective annual doses assessed by means of two models: dosimetric and epidemiological for the general population and hard working men. In the tested houses the radon concentrations ranges from 19 to 1668 Bq/m^3 with an arithmethic mean of 300 Bq/m^3 (geometric mean of 140 Bq/m^3, median of 103 Bq/m^3). In five houses radon concentration exceeds 1000 Bq/m^3, in eight houses it falls in the limits of 400 to 1000 Bq/m^3 and in forty three houses it is below 400 Bq/m^3 – the upper limit recommended by the European Union in "older" dwellings. The values of the PAEC range from 64 to 3805 nJ/m^3. The fraction of the unattached fraction f_p changes from below the detection limit of 0.2 to 53% with an arithmethic mean

of 17% (geometric mean of 12% and median of 17%). The highest values, above 30%, were detected in four rural houses well ventilated during absence of anybody in the room. The equilibrium factor F ranges from 8 to 64% with an arithmetic mean of 32% (geometric mean of 27% and median of 29%). A. Reineking and J. Porstendorfer found close mean value of 30% for F and a bit less of ca. 10% for f_p in their studies [12]. Although the observed range of the factor F is rather wide but the arithmetic mean of 32% is in a pretty good agreement with the value of 40% recommended in the routine estimations of the PAEC on the basis of the radon concentration measurements [2, 19]. The highest values of the factor F, above 60%, were measured in seven cases in the conditions of boiling, frying or smoking cigarettes. Thus, normally the high values of the factor F are not permanent, they correspond rather to short-lived activities.

The differences between the values of the doses estimated by the two models depend on the fraction of the unattached fraction f_p. According to the dosimetric models, the dose conversion factors increase nearly linearly with the unattached fraction f_p. Therefore, the dependence of the ratios of the dosimetric to epidemiological doses on the value of f_p, shown in Fig. 5, is also well described as linear. The ratios fall in the limits between 0.6 and 1.7 with an arithmetic, geometric mean and median equal to 1.0 for the general population and of 0.8 to 2.6 with an arithmetic, geometric mean and median equal to 1.4 for the hard working adult male. In Fig. 5 it can be seen that the epidemiological doses are underestimated compared to the dosimetric doses up to 1.7 times for the general population and up to 2.6 times in case of the hard working men. S. B. Solomon received similar results for guides in Fairy Cave in Australia [15]. He estimated that the radon dose to which the guides are exposed during work, if calculated as an epidemiological dose, is underestimated ca. two times compared to a dosimetric one.

It is worthy of underling that the value of the breathing rate admitted in the calculation is of significant influence on the resulting dose. There are suggestions that for the hard working men the breathing rate value of 1.7 m^3/h should be admitted rather than 1.2 m^3/h [19].

In Fig. 6 the courses in time of C_{Rn}, PAEC, F, f_p, HE Occ, HE Env doses, HE Occ/D Occ and HE Env/D Env

$y = 0,03x + 0,82$
$R^2 = 0,91$

$y = 0,02x + 0,64$
$R^2 = 0,85$

♦ HE Env/D1.1
■ HE Occ/D1.4
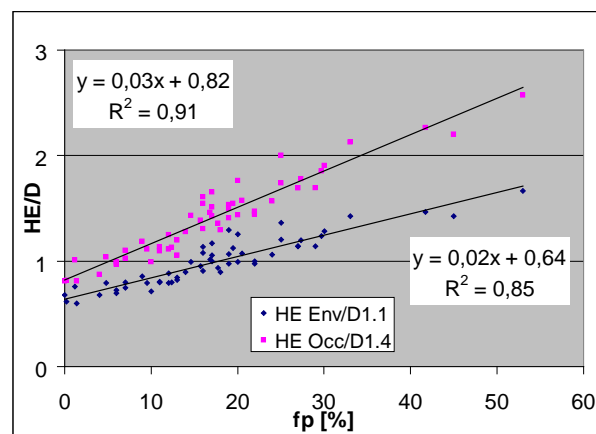
Fig. 5. Ratios of the dosimetric to epidemiological dose estimates vs. the unattached fraction f_p.
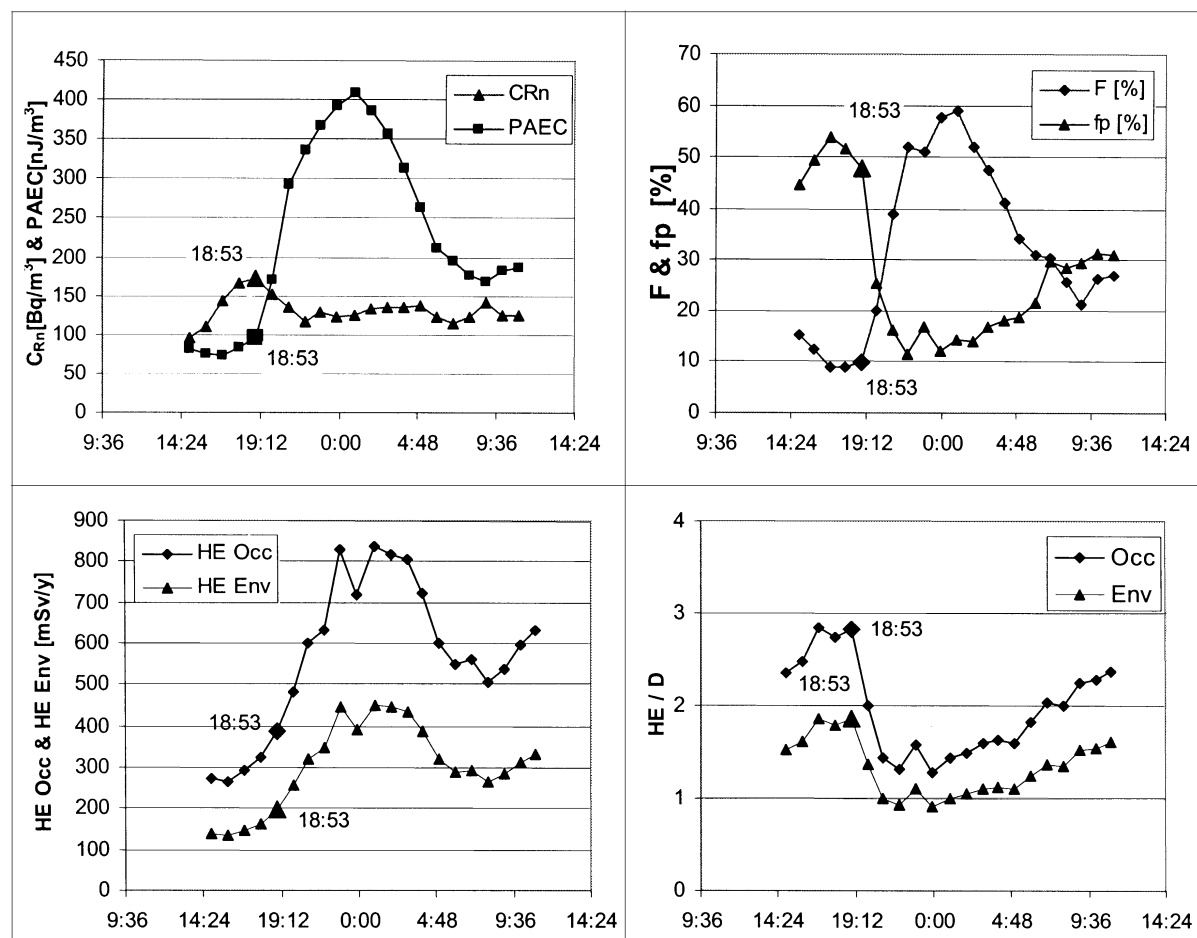
Fig. 6. Courses in time of C_{Rn}, PAEC, F, f_p, HE Occ, HE Env and ratios of HE/D in a house in Warsaw. At ca. 19:00 a cigarette was smoked.

ratios during longer measurement in a Warsaw house are plotted. It can be seen that at ca. 19:00 inhabitants smoked cigarettes what caused an increase in the PAEC from 100 nJ/m³ to 400 nJ/m³, in the equilibrium factor F from 10 to 58%, and in the annual dose from ca. 200 mSv to ca. 450 mSv (for population) and a drop in the f_p from 48 to 15% and in the ratio of the two dose estimates from 1.8 to 1 (for population).

Outdoors

It was planned to make measurements also nearby all the investigated houses. But only in four sites, all in the Sudety region, the counting statistics was high enough to deliver reliable results.

In Table 5 there are modes in the particle size distributions outdoors. In three cases there are just two modes with a mean of the GMD of 0.8 nm for the unattached fraction and 175 nm for the attached fraction. In the fourth case the attached fraction has two modes: 138 nm (79%) and 814 nm (9%). The mean contribution of the unattached fraction (mode #1) is 19%. In Table 6 there are results of f_p, PAEC, C_{Rn}, both kinds of doses HE Env and D Env, HE Occ and D Occ and the ratios of the dosimetric to the epidemiological dose for the hard working and general population. Values of the f_p and F range from 12 to 31% and from 6 to 33%, respectively. The mean ratio of the two doses for the general population and hard working men is equal to 1.0 and 1.4, respectively, the same as for the indoor results.

Table 5. The particle size distributions outdoors

Name of place	Mode #1			Mode #2			Mode #3		
	GMD[a] (nm)	GSD[b]	U[c] (%)	GMD (nm)	GSD	U (%)	GMD (nm)	GSD	U (%)
Przesieka	0.8	0.6	19	195	1.9	81	–	–	–
Borowice	0.7	1.3	14	138	2.9	86	–	–	–
Kurosiówka	0.8	1.4	31	229	2.5	69	–	–	–
Janowice Wlk.	0.7	1.2	12	138	1.4	79	814	1.2	9.0
Arithmetic mean	**0.8**	**1.1**	**19**	**175**	**2.2**	**79**			

[a] GMD – geometric mean diameter.
[b] GSD – geometric standard deviation.
[c] U – percentage contribution.

Table 6. Results of the measurements and calculations in four outdoors sites

Name of place	f_p (%)	F (%)	PAEC (nJ/m³)	C_{Rn} (Bq/m³)	HE Env (mSv/y)	D Env (mSv/y)	HE Env/ D Env	HE Occ (mSv/y)	D Occ (mSv/y)	HE Occ/ D Occ
Przesieka	19	33	144	79	1.31	1.39	0.94	2.48	1.80	1.38
Borowice	14	31	201	116	2.10	1.94	1.08	3.80	2.51	1.51
Kurosiówka	31	17	77	83	0.87	0.74	1.17	1.70	0.96	1.77
Janowice Wlk.	12	6	28	82	0.21	0.27	0.80	0.39	0.35	1.11
Arithmetic mean	**19**	**22**	**113**	**90**	**1.1**	**1.1**	**1.0**	**2.1**	**1.4**	**1.4**

Conclusions

The experimental material collected during the measurements in 56 dwellings in various conditions of the radon and aerosol concentrations leads to the following conclusions:

– The unattached fraction f_p and equilibrium factor F stay in broad ranges from nearly 0 to 53% with a mean of 18% and 8 to 64% with a mean of 32%, respectively and are influenced by the behaviour of the inhabitants, such as, e.g. cooking or smoking cigarettes (Fig. 6). When a cigarette was lit in the Warsaw
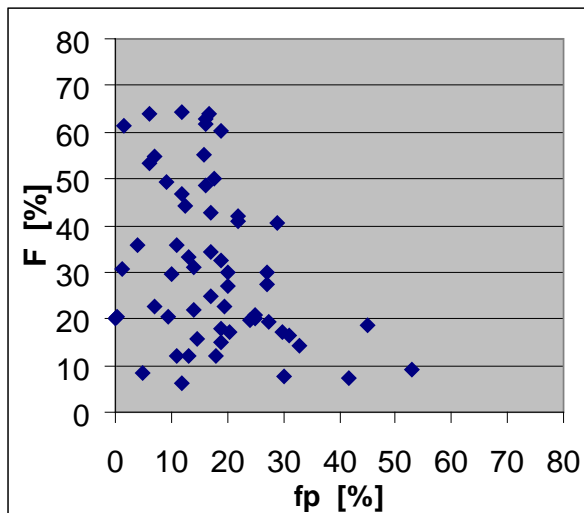
Fig. 7. The relations: F vs. f_p for the indoor and outdoor results.
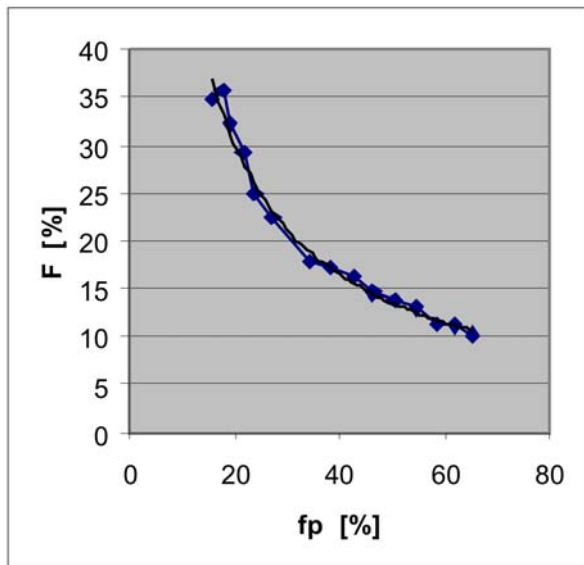
Fig. 8. The equilibrium factor F vs. the unattached fraction f_p, in the CLOR radon chamber.

house the PAEC, the equilibrium factor F and the annual dose increased four, six and two and half times, respectively. The unattached fraction f_p and the ratio of the two dose estimates decreased ca. 3 and ca. 2 times, respectively. The highest values of the factor F were found during cooking or smoking.

– In natural domestic conditions a negative correlation between the equilibrium factor F and the unattached fraction f_p corresponding to many various houses is not observed, as it is illustrated in Fig. 7, on the contrary to the artificial conditions in the radon chamber (Fig. 8). The difference can result from the different conditions of deposition and ventilation in various natural domestic environment, while they are stable in the chamber.

– Since according to the dosimetric models the dose conversion factors increase nearly linearly with the unattached fraction f_p, the dependence of the ratios of the dosimetric to epidemiological doses on the unattached fraction is also well described by a linear equation, as it is shown in Fig. 5.

– An arithmetic mean of the ratios of the dosimetric to epidemiological dose estimates for the general population is 1.0 and for the working men is 1.4.

Summary

In general, there is a quite good agreement between values of the effective doses estimated by means of so radically different approaches, but we should remember that all values of the dosimetric dose estimates in the above calculations were obtained with the use of a factor of 0.3 to match the RADEP-derived DCF values to the ICRP 65 conversion convention [5]. Thus, a question arises if the two different approaches can be reconciled. J. Stather [16] examined the main factors underlying the discrepancy between the two approaches and he indicated that the tissue and radiation weighting factors, admitted as $w_T = 0.12$ and $w_R = 20$, may substantially influence this discrepancy. However, the 2007 ICRP new recommendations (Publication 103) [7] maintained the same values for w_T and w_R.

On the basis of the more recent miner epidemiological studies on the risks at low levels of the radon exposure Publication 103 provides updated values of detriment per unit effective dose for low level exposure: 4.2×10^{-5}/mSv for workers and 5.7×10^{-5}/mSv for the general public [11]. Using these values together with the revised risk coefficient of 5×10^{-4}/WLM[a] the new values of the radon progeny conversion

---

[a] WLM (working level month) is a traditional unit of exposure to radon daughters. 1 WLM = 12.97 J·s·m⁻³.

convention, are recommended. They are 9 mSv/WLM (ca. 2500 mSv/(J·h·m^{-3})) instead of 4 mSv/WLM for members of the public and 12 mSv/WLM (ca. 3333 mSv/(J·h·m^{-3})) instead of 5 mSv/WLM (1425 mSv/(J·h·m^{-3})) for workers. The new values of the conversion conventions are ca. 2.3 times higher than the previous ones what makes the results of the two approaches remarkably closer.

References

1. Birchall A, James AC (1994) Uncertainty analysis of the effective dose per unit exposure from radon progeny and implications for ICRP risk-weighting factor. Radiat Prot Dosim 53;1/4:133–140
2. Cavallo A (2000) The radon equilibrium factor and comparative dosimetry in homes and mines. Radiat Prot Dosim 92;4:295–298
3. Cheng YS, Keating JA, Kanapilly GM (1980) Theory and calibration of screen type diffusion battery. J Aerosol Sci 11:549–556
4. Cheng YS, Yeh HC (1980) Theory of screen type diffusion battery. J Aerosol Sci 11:313–319
5. International Commission on Radiological Protection (1993) Protection against Radon-222 at home and at work. ICRP Publication 65, Ann ICRP 23(2)
6. International Commission on Radiological Protection (1994) Human respiratory tract model for radiological protection. ICRP Publication 66, Ann ICRP 24(1–3)
7. International Commission on Radiological Protection (2007) The 2007 recommendations of the International Commission on Radiological Protection. ICRP Publication 103, Ann ICRP 37(2–4)
8. James AC, Birchall A (1995) New ICRP lung dosimetry and its risk implications for alpha emitters. Radiat Prot Dosim 60;4:321–326
9. Maher EF, Laird NM (1985) Algorithm reconstruction of particle size distributions from diffusion battery data. J Aerosol Sci 16:557–570
10. Marple VA, Rubow KL (1986) Theory and design guidelines, cascade impactors: Sampling of data. Chapter 4. In: Lodge JP, Chan TL (eds) Cascade impactor: samplying and data analysis. American Industrial Hygiene Association, Akron, OH
11. Marsh JW, Harrison JD, Laurier D, Blanchardon E, Paquet F, Tirmach M (2010) Dose conversion factors for radon: recent developments. Health Phys 99;4:511–516
12. Reineking A, Porstendorfer J (1990) "Unattached" fraction of short-lived Rn decay products in indoor and outdoor environments: an improved single-screen method and results. Health Phys 58;6:715–725
13. Solomon SB (1997) A radon progeny sampler for the determination of effective dose. Radiat Prot Dosim 72:31–42
14. Solomon SB (1999) Manual for Radon Progeny Particle Size Spectrometer (RPPSS) Mk2. ARPANSA, Yallambie, Australia
15. Solomon SB (2001) Field tests of a radon progeny sampler for the determination of effective dose. Sci Total Environ 272:303–313
16. Stather JW (2004) Dosimetric and epidemiological approaches to assessing radon doses – can the differences be reconciled. Radiat Prot Dosim 112;4:487–492
17. Twomey S (1975) Comparison of constrained linear inversion and iterative algorithm appllied to the indirect estimation of the particle size distribution. J Comput Phys 18:188–200
18. Wąsiołek PT, Hopke PK, James AC (1992) Assessment of exposure to radon decay products in realistic living conditions. J Exposure Anal Environ Epidemiol 2;3:309–322
19. Zock C, Porstendorfer J, Reineking A (1996) The influence of biological and aerosol parameters of inhaled short-lived radon decay products on human lung dose. Radiat Prot Dosim 63;3:197–206